journal homepage: www.intl.elsevierhealth.com/journals/cmpb

Reprint of "Pharmacokinetic modelling of the anti-malarial drug artesunate and its active metabolite dihydroartemisinin"☆,☆☆

Adam J. Hall[a,*], *Michael J. Chappell*[b], *John A.D. Aston*[c], *Stephen A. Ward*[d]

[a] *Departments of Mathematics and Statistics, University of Warwick, Gibbet Hill Road, Coventry CV4 7AL, UK*
[b] *School of Engineering, University of Warwick, Gibbet Hill Road, Coventry CV4 7AL, UK*
[c] *Department of Statistics, University of Warwick, Gibbet Hill Road, Coventry CV4 7AL, UK*
[d] *Liverpool School of Tropical Medicine, Pembroke Place, Liverpool L3 5QA, UK*

ARTICLE INFO

Article history:
Received 6 December 2012
Received in revised form
15 April 2013
Accepted 15 May 2013

Keywords:
Mathematical models
Biomedical systems
Drug kinetics
Structural identifiability
Parameter estimation
Sensitivity analysis

ABSTRACT

A four compartment mechanistic mathematical model is developed for the pharmacokinetics of the commonly used anti-malarial drug artesunate and its principle metabolite dihydroartemisinin following oral administration of artesunate. The model is structurally unidentifiable unless additional constraints are imposed. Combinations of mechanistically derived constraints are considered to assess their effects on structural identifiability and on model fits. Certain combinations of the constraints give rise to locally or globally identifiable model structures.

Initial validation of the model under various combinations of the constraints leading to identifiable model structures was performed against a dataset of artesunate and dihydroartemisinin concentration–time profiles of 19 malaria patients. When all the discussed constraints were imposed on the model, the resulting globally identifiable model structure was found to fit reasonably well to those patients with normal drug absorption profiles. However, there is wide variability in the fitted parameters and further investigation is warranted.

1. Introduction

Malaria is a parasitic disease that has affected humans and animals for thousands of years [1]. Even now in the 21st century, the most deadly strain *Plasmodium falciparum* infects 200 million people and causes over half a million deaths every year, with young children being most severely affected [2].

Artemisinin and its derivatives have been used as anti-malarials with increasing frequency since the 1990s [3]. They are the most rapidly acting drugs out of the currently available anti-malarials [4], reducing the parasite biomass

DOI of original article:http://dx.doi.org/10.1016/j.cmpb.2013.05.010.

☆☆ This article is a reprint of a previously published article. For citation purposes, please use the original publication details "*Computer Methods and Programs in Biomedicine*" 112 (2013) 1–15.
* *Corresponding author*. Tel.: +44 24765 24309.
E-mail address: Adam.J.Hall@warwick.ac.uk (A.J. Hall).
0169-2607/$ – see front matter © 2013 Adam J. Hall. Published by Elsevier Ireland Ltd. All rights reserved.
http://dx.doi.org/10.1016/j.cmpb.2013.12.001

~10, 000-fold per asexual life cycle [5,4]. They are well-tolerated and produce few side-effects [4], and as such form the core part of the World Health Organisation recommended first-line treatment for many patients: artemisinin-based combination therapies [2]. Artemisinins remain as the most effective drugs to which malaria has not yet developed widespread resistance, though resistance has been confirmed in some regions [4]. It is hoped that use of these combination therapies, in favour of artemisinin monotherapies, will assist in delaying artemisinin resistance to ensure artemisinins continue to remain effective against multi-drug resistant malaria [4]. Meanwhile, there remains an urgent need to develop new antimalarials [6].

However, the behaviour of current artemisinins is still not fully understood; debate remains concerning their mechanism of action [7,8] and stage-specific effects [9]. One theory is that artemisinins decompose when activated by iron that has accumulated in malaria infected red blood cells, forming free radicals which then damage the parasites [10]. Thus in this theory, the anti-malarial action also acts as a route of elimination for artemisinins.

Further, recrudescence is frequently observed with the currently adopted dosing regimens [11], which have been derived largely empirically [4]. This recrudescence may be attributed to either resistant or arrested/dormant parasites, or the drug concentrations in blood falling below their effective levels, but such issues have not yet been fully characterised [9].

The blood plasma concentration–time profiles and thus the pharmacokinetics of artemisinins have been shown to display high inter-individual variability in the majority of studies. Further understanding of the pharmacokinetics and pharmacodynamics of artemisinins may assist in informing more effective dosing regimens, as well as the development of improved antimalarials. This work focusses on the pharmacokinetics because a pharmacodynamic model should build on a well-suited pharmacokinetic model.

Artesunate (hereafter ARS) is the most frequently used artemisinin derivative, and is rapidly and almost entirely converted to dihydroartemisinin (hereafter DHA) *in vivo*, mostly by plasma esterases and liver cytochrome P450 CYP2A6 [12–14]. DHA is the most active of all artemisinin derivatives, with activity approximately 1.4 times that of ARS [15].

ARS is water soluble, facilitating its absorption [16] (usually assumed to be fast, efficient and first-order [12]). Its rapid hydrolysis into the more active metabolite means that although ARS may make a significant contribution to parasite kill [17], it is often referred to as a pro-drug for DHA [3], and some researchers take the viewpoint that it is therefore not necessary to model the parent drug. DHA is also rapidly eliminated, again either through activation by infected red blood cells or through further metabolism (e.g. glucuronidation [4]), but the metabolites of DHA are inactive [18].

Many of the results and methods of studies involving ARS and DHA are summarised in Morris et al. [12], so no attempt is made to list them here. Instead, a brief discussion of existing models for artemisinin-class drugs in general, their features and the analyses conducted on them is provided in the next subsection.

1.1. *Existing models*

Many existing pharmacokinetic studies for artemisinins have been conducted over the last couple of decades, and have successfully provided some insights into the absorption, elimination and/or multiple dosing behaviour of these drugs, and the covariates that influence these. Some studies have restricted their interest to either healthy subjects, uncomplicated malaria, or severe malaria, and either children, adults or pregnant women, while others have been designed specifically to consider the differences between some of these groups. Each study focusses on a specific artemisinin derivative or derivatives, and a specific route or routes of administration, either alone or in combination with other antimalarial agents.

Of those that used modelling rather than non-compartmental approaches, some have been used to analyse the effects of differing dosing regimens in different contexts, including cases where the malaria has developed resistance to this class of drugs [19]. They range from being very simple, e.g. with linear absorption and exponential elimination as in Saralamba et al. [19], to being quite complicated, e.g. involving 9 compartments as in Gordi et al. [20], and of various complexities in between, e.g. 4 compartments as in Tan et al. [21].

However, such models have not been analysed to determine if they are structurally identifiable. The importance of knowing the structural identifiability of models will be reiterated in this paper. Indeed, Karunajeewa et al. [22] use a three-compartment model based on mechanistic principles but experience problems obtaining parameter estimates, perhaps due to structural identifiability issues. In many of the more complicated models, there are even more unknown parameters and many of these have to be assigned fixed values in order to estimate the remaining parameters successfully (again perhaps due to structural identifiability issues). In those cases, the selection of the parameters to fix and what values to use can be somewhat arbitrary and the effects of using other values is not always explored or reported.

When processes involved in the system being modelled are not well understood, it can be informative to perform model selection based on comparing a relative goodness of fit statistic for a variety of structural models, and indeed this approach is used to various extents for the pharmacokinetic models used for artemisinins in the literature. However, when information is known about the processes and mechanisms involved, models selected in this way can be less useful than models of process [23], and of course different models must be used for different observational situations (e.g. Gordi et al. [20] measure drug concentrations in saliva samples as opposed to the more common use of plasma samples, and so uses a model tailored for that situation). To be fully certain of model appropriateness, fits should be reported and validated on an individual patient basis in addition to any population levels of interest. (If a mixed-effects/hierarchical model is used, this means estimating the subject-specific deviation from the mean parameters.) This can help to determine whether or not there are key features of the data that are missed due to the structure of the model employed, which may go unnoticed if only population data are considered. However, pharmacokinetics on an individual patient basis are understandably of

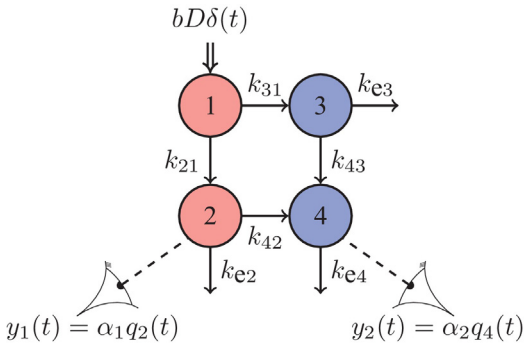

Fig. 1 – System diagram of the general compartmental model

less interest than at population levels, and so attention typically focusses only on population fits.

In summary, there are currently no known coupled mechanistic pharmacokinetic models for artemisinin derivatives and corresponding metabolites *in vivo*, with observations made of the blood plasma concentrations of the administered derivatives and their metabolites, that have either been analysed in a structural identifiability sense or validated on an individual patient basis.

2. The model

A relatively simple coupled mechanistic model was developed for the pharmacokinetics of orally-administered ARS and its principle metabolite DHA, for situations where blood plasma concentrations of both are observed, and is depicted in Fig. 1.

It consists of four linked compartments, with the parent drug and its metabolite each represented by two compartments: an absorption (gut) compartment and a circulation/plasma compartment. The absorption compartments account for the delay in the drug and metabolite reaching the circulation (and site of measurement) due to the oral route of administration.

This differs structurally from the generic parent-metabolite model with oral dose described by Cheung et al. [24] (analysed for structural identifiability and applied to dextromethorphan and dextrophan), which uses an extra peripheral compartment for the parent drug and has a direct flow from its single absorption compartment to the observed/central metabolite compartment.

The administered oral dose of ARS is considered as a bolus (impulsive) input into its absorption compartment (1 in the diagram). To account for bioavailability, a fraction b of the administered dose D is assumed to reach the systemic circulation. The dose D is prescribed in proportion to the body weight of the patient, and so taken in units of nmol per kg.

Once in the system, ARS is either irreversibly metabolised into DHA (compartment 3) prior to reaching the circulation (compartment 4), or is absorbed into the circulation (compartment 2) and subsequently metabolised (compartment 4 again). Elimination can occur from any compartment except the input compartment, and can be caused by either excretion from the body or further metabolism into inactive metabolites which are not of interest.

Observations are made of the drug concentrations in the circulation compartments, with observation gains α_1 for ARS (y_1) and α_2 for DHA (y_2). These parameters incorporate the volumes of distribution of the respective drugs. As is standard for the purposes of assessing the identifiability of the structural model, it is assumed that observations are made continually over the entire infinite time horizon, and are made without error. These two assumptions are relaxed later when dealing with the problem of parameter estimation from data.

Note that because metabolism of ARS into DHA takes place in the liver as well as in esterases, metabolism can occur before presentation in the observed circulation compartments. Indeed, in concentration–time profiles of malaria patients (e.g. those analysed in this work), large quantities of DHA are observed in the blood plasma prior to those of ARS, which cannot be attributed solely to being artefacts of differing observation gains (or otherwise to quantification limits). Hence, the presence of compartment 3 is crucial to capture the metabolism-before-absorption route that ARS can take.

The differential equation characterisation of the model is given, for $t \in [0, \infty)$ describing the time in hours since drug administration, by

$$\begin{cases} \mathbf{q}'(t) &= \mathbf{A}\mathbf{q}(t) + \mathbf{B}\mathbf{u}(t) \\ \mathbf{q}(0^+) &= \mathbf{q}_0 \\ \mathbf{y}(t) &= \mathbf{C}\mathbf{q}(t). \end{cases} \tag{1}$$

Here, $\mathbf{q} = (q_1\, q_2\, q_3\, q_4)^{\mathrm{T}}$ represents the state vector of the system model, where each q_i denotes the quantity of the respective drug in compartment i, $\mathbf{u}(t) = (D\delta(t)\,0\,0\,0)^{\mathrm{T}}$ denotes the model input and $\mathbf{q}_0 = (0\,0\,0\,0)^{\mathrm{T}}$ the initial condition, $\mathbf{y}$ denotes the vector-valued observation function, and the model matrices are

$$\mathbf{A} = \begin{pmatrix} -(k_{21}+k_{31}) & 0 & 0 & 0 \\ k_{21} & -(k_{42}+k_{e2}) & 0 & 0 \\ k_{31} & 0 & -(k_{43}+k_{e3}) & 0 \\ 0 & k_{42} & k_{43} & -k_{e4} \end{pmatrix}, \tag{2a}$$

$$\mathbf{B} = \begin{pmatrix} b \\ 0 \\ 0 \\ 0 \end{pmatrix}, \quad \mathbf{C} = \begin{pmatrix} 0 & \alpha_1 & 0 & 0 \\ 0 & 0 & 0 & \alpha_2 \end{pmatrix}. \tag{2b}$$

Note that there are different ways to parameterise $\mathbf{u}$, $\mathbf{q}_0$ and $\mathbf{B}$. The parameterisation used here has been chosen as it more clearly corresponds to the mechanistic concepts.

Due to the difference in the molecular weights of the parent drug and the metabolite, the q_i are considered in units of molar mass, per kilogram of patient body weight (nmol/kg). Observations, which are concentrations, are assumed to be in units of nmol/l. The observation gains α_1 and α_2 therefore have units of kg/l, but the volumes of distribution are generally assumed to

scale approximately linearly with patient body weight, hence the reason that the dosing is calculated in those terms.

All flows (absorption, metabolism and elimination) are assumed to be first-order and linear, with rate constants k_{ij} (denoting the flow rate constant to compartment i from compartment j, or to the environment when $i = e$) time-invariant and specified in units of per hour (which are standard units for artemisinin drugs). Note that conversion into inactive unmeasured metabolites and excretion from the body are considered as flows to the environment with respect to the system model.

The system of equations (1), with $\mathbf{u}(t)$ and $\mathbf{q}_0$ as described above, can easily be solved analytically to yield:

$$\mathbf{q}(t) = bDe^{\mathbf{A}t}, \quad \mathbf{y}(t) = \mathbf{C}\mathbf{q}(t). \tag{3}$$

The solution for the state variables is thus

$$\begin{aligned}
q_1(t) &= bDe^{-(k_{21}+k_{31})t} \\
q_2(t) &= \frac{bDk_{21}\left(e^{-(k_{42}+k_{e2})t} - e^{-(k_{21}+k_{31})t}\right)}{k_{21}+k_{31}-k_{42}-k_{e2}} \\
q_3(t) &= \frac{bDk_{31}\left(e^{-(k_{43}+k_{e3})t} - e^{-(k_{21}+k_{31})t}\right)}{k_{21}+k_{31}-k_{43}-k_{e3}} \\
q_4(t) &= bD\left(e^{-(k_{21}+k_{31})t}\right. \\
&\quad \frac{k_{21}^2k_{42}+k_{31}k_{43}(k_{31}-k_{42}-k_{e2})+k_{21}(k_{31}(k_{42}+k_{43})-k_{42}(k_{43}+k_{e3}))}{(k_{21}+k_{31}-k_{42}-k_{e2})(k_{21}+k_{31}-k_{43}-k_{e3})(k_{21}+k_{31}-k_{e4})} \\
&\quad - \frac{e^{-(k_{42}+k_{e2})t}k_{21}k_{42}}{(k_{21}+k_{31}-k_{42}-k_{e2})(k_{42}+k_{e2}-k_{e4})} \\
&\quad - \frac{e^{-(k_{43}+k_{e3})t}k_{31}k_{43}}{(k_{21}+k_{31}-k_{43}-k_{e3})(k_{43}+k_{e3}-k_{e4})} \\
&\quad \left. + \frac{e^{-k_{e4}t}(k_{31}k_{43}(k_{42}+k_{e2}-k_{e4})+k_{21}k_{42}(k_{43}+k_{e3}-k_{e4}))}{(k_{21}+k_{31}-k_{e4})(k_{42}+k_{e2}-k_{e4})(k_{43}+k_{e3}-k_{e4})}\right).
\end{aligned} \tag{4}$$

3. Structural identifiability

Before attempting to apply this model to real data for parameter estimation, it is necessary to check that all the parameters are theoretically identifiable from "perfect data" (noise-free data available over the entire infinite time horizon assuming no model misspecification), in the sense that they can either be uniquely determined or there are only a countable number of alternative parameter combinations with identical input/output structure. This is the structural identifiability property, and is an important property to check in order to understand what kinds of inferences can validly be made about the parameters in the model. For an unidentifiable model, a good fit to data does not imply that the estimated parameters have any connection to the intended interpretations, which may invalidate model predictions and in turn cause important decisions in terms of dosing regimens to be made incorrectly.

Let $\mathbf{p}$ denote the vector of unknown parameters in the model. Take

$$\mathbf{p} = \begin{pmatrix} b & k_{21} & k_{31} & k_{42} & k_{43} & k_{e2} & k_{e3} & k_{e4} & \alpha_1 & \alpha_2 \end{pmatrix}^{\mathrm{T}}, \tag{5}$$

where the feasible parameter space is $\Omega := (0, \infty)^n \ni \mathbf{p}$, with $n = 10$ denoting the number of unknown parameters.

The observation function $\mathbf{y}$ is now written $\mathbf{y}(\cdot, \mathbf{p})$ to emphasise its dependence on the unknown parameters.

3.1. Structural identifiability definitions

Structural identifiability is the measure theoretic concept of local injectivity of the observation function with respect to the model parameters, excepting sets of parameter values with measure zero.

A component parameter p_i of $\mathbf{p}$ is said to be

- structurally locally identifiable (SLI) iff for almost every $\mathbf{p} \in \Omega$, there exists a neighbourhood $N(\mathbf{p}) \subseteq \Omega$ of vectors around $\mathbf{p}$ such that

$$\begin{aligned}
&\text{if } \bar{\mathbf{p}} \in N(\mathbf{p}) \text{ and } \mathbf{y}(\cdot, \mathbf{p}) = \mathbf{y}(\cdot, \bar{\mathbf{p}}) \\
&\text{then } \bar{p}_i = p_i;
\end{aligned} \tag{6}$$

- structurally unidentifiable (SUI) otherwise.

If $N(\mathbf{p}) = \Omega$ can be used in (6) for almost every $\mathbf{p}$, then p_i is also said to be *structurally globally identifiable (SGI)*.

The structural identifiability of the whole model is defined in terms of the structural identifiability of the unknown parameters as follows:

- The model is *structurally locally identifiable* iff **all** parameters in $\mathbf{p}$ are at least structurally locally identifiable;
- The model is *structurally unidentifiable* iff **any** of the parameters in $\mathbf{p}$ are structurally unidentifiable.

If **all** the parameters in the model are also structurally globally identifiable then the model itself is said to be structurally globally identifiable.

Note that structural identifiability depends on each of the feasible parameter space, the system model structure, the observations and the inputs.

3.2. Analysis for present model

The structural identifiability of this model was analysed using the Laplace transform approach [25], one of the most commonly used methods for linear time-invariant systems.

This method considers the Laplace transforms of the observation functions after eliminating the state variables. It extracts the coefficients of the resulting expressions once written in a standard form, with common factors in each respective numerator and denominator cancelled. These coefficients are assembled in a vector $\Phi(\mathbf{p})$ as an "exhaustive summary" of observational parameters [26]. The injectivity condition of the full observation function vector is equivalent to that of the exhaustive summary, and the latter has the advantage of being easier to work with.

The Laplace transforms of the observation functions $y_1(\cdot, \mathbf{p})$ and $y_2(\cdot, \mathbf{p})$ are given (in their simplest forms), for $s \in \mathbb{C}$, by

$$Y_1(s, \mathbf{p}) = \frac{\phi_1(\mathbf{p})}{s^2 + \phi_2(\mathbf{p})s + \phi_3(\mathbf{p})}, \tag{7a}$$

$$Y_2(s,\mathbf{p}) = \frac{\phi_4(\mathbf{p})s + \phi_5(\mathbf{p})}{s^4 + \phi_6(\mathbf{p})s^3 + \phi_7(\mathbf{p})s^2 + \phi_8(\mathbf{p})s + \phi_9(\mathbf{p})}, \tag{7b}$$

where the coefficients depending on $\mathbf{p}$ form the exhaustive summary and are given by

$$\phi_1(\mathbf{p}) = \alpha_1 bDk_{21} \tag{8a}$$

$$\phi_2(\mathbf{p}) = k_{21} + k_{31} + k_{42} + k_{e2} \tag{8b}$$

$$\phi_3(\mathbf{p}) = (k_{21} + k_{31})(k_{42} + k_{e2}) \tag{8c}$$

$$\phi_4(\mathbf{p}) = \alpha_2 bD(k_{21}k_{42} + k_{31}k_{43}) \tag{8d}$$

$$\phi_5(\mathbf{p}) = \alpha_2 bD(k_{21}k_{42}(k_{43} + k_{e3}) + k_{31}k_{43}(k_{42} + k_{e2})) \tag{8e}$$

$$\phi_6(\mathbf{p}) = k_{21} + k_{31} + k_{42} + k_{43} + k_{e2} + k_{e3} + k_{e4} \tag{8f}$$

$$\phi_7(\mathbf{p}) = (k_{21} + k_{31})(k_{42} + k_{43} + k_{e2} + k_{e3} + k_{e4}) + k_{e4}(k_{42} + k_{43} + k_{e2} + k_{e3}) + (k_{42} + k_{e2})(k_{43} + k_{e3}) \tag{8g}$$

$$\phi_8(\mathbf{p}) = k_{e4}(k_{21}(k_{42} + k_{43} + k_{e2} + k_{e3}) + k_{31}(k_{42} + k_{43} + k_{e2} + k_{e3}) + (k_{42} + k_{e2})(k_{43} + k_{e3})) + (k_{21} + k_{31})(k_{42} + k_{e2})(k_{43} + k_{e3}) \tag{8h}$$

$$\phi_9(\mathbf{p}) = k_{e4}(k_{21} + k_{31})(k_{42} + k_{e2})(k_{43} + k_{e3}). \tag{8i}$$

Using the Laplace transform approach, the structural (local) identifiability problem is to determine whether, for generic $\mathbf{p}$, the only solution (in a neighbourhood of $\mathbf{p}$) to the system of equations

$$\phi_1(\mathbf{p}) = \phi_1(\bar{\mathbf{p}}) \tag{9a}$$

$$\phi_2(\mathbf{p}) = \phi_2(\bar{\mathbf{p}}), \tag{9b}$$

$$\vdots \tag{9c}$$

$$\phi_9(\mathbf{p}) = \phi_9(\bar{\mathbf{p}}) \tag{9d}$$

is

$$\mathbf{p} = \bar{\mathbf{p}}. \tag{10}$$

The symbolic computer package Maple (version 16) was used to solve this system of equations. Mathematica (version 8.0.1) failed to solve this system of equations on an Intel Core i5 2.40 GHz machine with 2.8 GB of memory before exhausting the available memory after 30 min, whereas Maple comfortably solved the system within 2 min on the same machine.

It is readily observed (e.g. from the Laplace coefficients) that b, α_1 and α_2 are not structurally identifiable individually, since they appear only as the products $b\alpha_1$ and $b\alpha_2$. In what follows, $b\alpha_1$ and $b\alpha_2$ are therefore considered to be combined parameters. Hence, the set of unknown parameters is now taken as

$$\mathbf{p} = (\,k_{21}\quad k_{31}\quad k_{42}\quad k_{43}\quad k_{e2}\quad k_{e3}\quad k_{e4}\quad b\alpha_1\quad b\alpha_2\,)^{\mathrm{T}},$$

(so with $n = 9$ unknown parameters) and the structural identifiability analysis proceeds in this setting.

Solving the system of equations (3.2) reveals that k_{e4} is SLI with either $\overline{k_{e4}} = k_{e4}$ or $\overline{k_{e4}} = k_{43} + k_{e3}$, and all other model parameters are SUI. As there is little point working with a SUI model, the following additional assumptions were therefore considered to see if they constrain the system model to be structurally identifiable:

1. Other studies have reported apparent volumes of distribution for ARS and DHA following oral administration of ARS. In particular, Morris et al. [12] report the median volume of distribution for ARS at 6.8 l/kg and 1.55 l/kg for DHA in malaria patients (though these are noted to vary significantly relative to severity of infection). Such information can be used to treat the ratio of the observation gains as known; that is, $r := \alpha_2/\alpha_1$ is known ($\alpha_1 = \alpha$ and $\alpha_2 = r\alpha$, say). Using the above information from Morris et al. [12], this would give $r = 4.387$ (the observation gain for DHA is larger because it has the smaller volume of distribution);
2. There is no known reason to suggest that the metabolism of the ARS occurs at significantly different rates before and after absorption, so it might be valid to consider the metabolism rate constants to be equal: $k_{31} = k_{42}$;
3. ARS is almost entirely converted to DHA (there are little excreted traces of ARS or its other metabolites), so it may be reasonable to assume that the elimination rate parameter $k_{e2} = 0$;
4. Absorption of the metabolite is rapid, thus its elimination may be negligible before it is absorbed, i.e. $k_{e3} = 0$.

Note that when constraints of this sort are imposed on parameters, the corresponding models are considered to be structurally distinct; structural identifiability is concerned with the behaviour of *almost all* parameter values, and these assumptions may mean that previously null sets now have strictly positive measure.

Each combination of these four assumptions was assessed using the same methods as previously, and the structural identifiability results are tabulated in Table 1. It can be seen that applying just one of the additional constraints does not improve the structural identifiability for the majority of the parameters. Applying any combination of two constraints except $\alpha_2/\alpha_1 = r$ and $k_{e2} = 0$ constrains all the parameters to be at least structurally locally identifiable. Applying any combination of three of the assumptions constrains the model to be structurally globally identifiable. The assumption (2) that $k_{31} = k_{42}$ seems to be the weakest in terms of improving structural identifiability.

Parameter estimates will be obtained with all four assumptions imposed, as it the strongest situation in terms of structural identifiability, and the fewer degrees of freedom will aid in more precise estimation of parameters. Parameter estimates will also be obtained with other structurally identifiable combinations of assumptions, to assess the sensitivity to the assumptions and to ensure that the system is not over-constrained.

Table 1 – Structural identifiability analysis results

Assumptions				Structural identifiability results									
$\frac{\alpha_2}{\alpha_1} = r$, r known	$k_{31} = k_{42}$	$k_{e2} = 0$	$k_{e3} = 0$	k_{21}	k_{31}	k_{42}	k_{43}	k_{e2}	k_{e3}	k_{e4}	$b\alpha_1$	$b\alpha_2$	$b\alpha$
0	0	0	0	U	U	U	U	U	U	L	U	U	–
0	0	0	1	U	U	U	L	U	–	L	U	U	–
0	0	1	0	U	U	L	U	–	U	L	U	U	–
0	0	1	1	L	L	L	L	–	–	L	L	L	–
0	1	0	0	U	–	U	U	U	U	L	U	U	–
0	1	0	1	L	–	L	L	L	–	L	L	L	–
0	1	1	0	G	–	G	L	–	L	L	G	L	–
0	1	1	1	G	–	G	G	–	–	G	G	G	–
1	0	0	0	U	U	L	U	L	U	L	–	–	U
1	0	0	1	L	L	L	L	L	–	L	–	–	L
1	0	1	0	U	U	G	U	–	U	G	–	–	U
1	0	1	1	G	G	G	G	–	–	G	–	–	G
1	1	0	0	L	–	L	L	L	L	L	–	–	L
1	1	0	1	G	–	G	G	G	–	G	–	–	G
1	1	1	0	G	–	G	G	–	G	G	–	–	G
1	1	1	1	G	–	G	G	–	–	G	–	–	G

The applicable parameters under any combination of the assumptions (1 if the assumption is applied and 0 if not) are either structurally unidentifiable (U), structurally locally identifiable (L) or structurally globally identifiable (G).

4. Parameter estimation

4.1. *Data*

The authors had access to a dataset of 19 malaria patients from a study carried out at the Department of Clinical Tropical Medicine, Faculty of Tropical Medicine, Mahidol University, Bangkok, 10400, Thailand. Patients were selected based on a diagnosis of adult non-severe *P. falciparum* malaria with a parasite count less than 10,000 parasites per microlitre of blood. The patients were each administered 2 mg/kg artesunate in fractions of 50 mg oral tablets (body weights not part of the dataset) twice daily for three days, in combination with 1800 mg fosmidomycin and 750 mg azithromycin which are antibiotics and not considered relevant to the modelling. Food was restricted for the first hour after dosing.

The data consist of ARS and DHA concentrations (provided in units of ng/ml but converted to nmol/l prior to analysis) from assayed blood plasma samples over a time course of 12 h. Blood plasma samples were drawn from the patients immediately after administration of the first dose on the first day, 15 min after, 30 min after, 1 h after, 1.5 h after, 2 h after, 3 h after, 4 h after, 6 h after, 8 h after and 12 h after administration of the first dose on the first day. No samples were taken for subsequent doses or on subsequent days and so cannot be included in the modelling.

Samples were analysed to determine their ARS and DHA concentrations using tandem liquid chromatography-mass spectrometry (on a Thermo Fisher Quantum Access Triple Quad Mass Spectrometer) based on the assay described in Lindegardh et al. [27]. (The individual samples were analysed only once but assay robustness was confirmed by a re-analysis of approximately 10% of all samples. Analytical runs included a full calibration curve and three replicate quality control samples.)

The assay has an associated *lower limit of quantification (LLOQ)* for each analyte and passed FDA validation, for which the requirement is to measure quality control samples and standard curve samples with known concentrations above the respective LLOQ to within ±15% of the nominal value. Specifically, the coefficient of variation for the assay is 15% for both analytes. Values below the respective LLOQ may have significantly greater relative uncertainty or noise. The LLOQ for ARS was $LLOQ_1 = 3.9$ nmol/l and that of DHA was $LLOQ_2 = 22.9$ nmol/l. The assumption is that values reported for unknown samples above the respective LLOQ will also be within 15% of the actual value. Observations below the respective LLOQ are felt to be so unreliable that such values are not quantified; they are only reported as being below the limit of quantification (BLQ). In this way, 41% of the ARS data and 8% of the DHA data are censored.

Note that over the 12 h time span for a single subject, a wide range of drug concentrations was observed, most particularly for DHA. Specifically, for DHA, concentrations smaller than the LLOQ and concentrations above 6000 nmol/l were recorded for some patients over the course of the sampling interval. In common with other studies, there was also wide variability between patients in terms of the concentration–time profiles for both ARS and DHA.

The majority of the patients had peak ARS concentrations within 1.5 h after drug administration (74%), and peak DHA concentrations within 2 h (63%). However, it was already clear from the data that over half of the patients experienced delayed or possibly double peaks in the concentration–time profiles for both ARS and DHA. These are not thought to be outliers due to the assay validation, and the pattern is quite consistent in some individuals. There are no covariates with these data to allow further analysis and the cause of this phenomenon is not known, nor the frequency of incidence in other artesunate studies as individual patient profiles are often not discernible. The only reference to this issue in relation to artemisinin drugs that the authors are aware of is to the derivative artemether, which was found by Van Agtmael et al. [28] to have a biphasic absorption profile. As the mechanistic

cause of the phenomenon is unknown, the differences in the absorption process have not been accounted for in the present model. This indicates that the model is misspecified and will not be suitable for all the patients, though it is hoped that it will still be applicable for many of the patients.

The patients were therefore divided into two groups, one where the concentration–time profiles for both ARS and DHA exhibited only a single peak each within the expected time after drug administration, and the other group for the remaining patients where the absorption profile was unexpected, e.g. being slower to reach the peak concentrations, having multiple peaks and/or having delayed elimination. Model fits and validation will therefore be separately described for each of the two groups.

For illustration, consider Fig. 2. The concentration–time profiles for both drugs for patient A were as expected, so this patient was placed in the first group. Patient B, however, clearly has an unusual concentration–time profile (and it is not clear whether it is just caused by random measurement error) and so was placed in the second group. The profiles for patient C exhibited later peaks (and thus delayed DHA elimination), and was also placed in the second group.

4.2. *Statistical treatment of data*

At this stage, the structural model is now considered **with error** (for a single patient), and the observations are now finite in number and collected at discrete times. Only measurement error is considered, as error resulting from model misspecification is assumed to be dominated by measurement error.

So, let $\tilde{y}_i$ denote the ith observation of drug d_i (0 = ARS, 1 = DHA) and t_i denote the time at which this observation was made. Then,

$$\tilde{y}_i = h_i(\mathbf{p}) + \epsilon_i,$$

where $h_i(\mathbf{p}) = \max\{y_{d_i}(\mathbf{p}, t_i), LLOQ_{d_i}\}$ is the model prediction of the ith observation and ϵ_i denotes the observation error (and y_{d_i} is as in (1)).

Statistically, it is assumed that the measurement error is normally distributed, so a measured value of $\tilde{y}_i$ is assumed to be an observation from a $N(h_i(\mathbf{p}), \sigma_i^2)$ distribution where $\sigma_i = \delta h_i(\mathbf{p})$ with $\delta = 0.15$. Equivalently, $\epsilon_i \sim N(0, \sigma_i^2)$. It is further assumed that the observation errors for observations at different times are independent. (This assumption may not be realistic but was felt to be a good starting point in the absence of any prior information to the contrary.) Observation errors for ARS and DHA observations obtained at the same time are assumed to be correlated with correlation parameter ρ unknown.

Note that this error model does not account for the fact that the observed concentrations will always be positive, but is nevertheless convenient to work with.

Observations below the respective LLOQ may be caused by no drug being present at all, the drug quantity being close to the LLOQ itself, or any range in between. Values below the LLOQ are treated as being *at* the LLOQ here, as this simplifies their statistical treatment, and this method was shown to pass certain tests for suitability, described shortly.

It is convenient to view the $\tilde{y}_i$ as forming a one-dimensional vector. Write $\tilde{\mathbf{y}}$ for the data and $\mathbf{h}(\mathbf{p})$ for their model predictions. The above specification gives rise to the following log-likelihood function, defined up to an additive arbitrary constant:

$$\ell(\mathbf{p}|\tilde{\mathbf{y}}) = -\frac{1}{2}\Big(\log\det \mathbf{V}(\mathbf{p}) + \underbrace{(\tilde{\mathbf{y}} - \mathbf{h}(\mathbf{p}))^{\mathrm{T}}\mathbf{V}(\mathbf{p})^{-1}(\tilde{\mathbf{y}} - \mathbf{h}(\mathbf{p}))}_{\text{weighted residual sum of squares (WRSS)}}\Big), \tag{11}$$

where $\mathbf{V}(\mathbf{p})$ is the weighting matrix with (i, i)-th element σ_i^2 and (i, j)-th element $\rho\sigma_i\sigma_j$ when $t_i = t_j$, $i \neq j$. Note that with this definition, the residuals $\tilde{y}_i - h_i(\mathbf{p})$ are zero for those points i where the model prediction and corresponding datum both lie below the LLOQ.

Similarly to Bergstrand and Karlsson [29], this methodology was first tested on simulated data to determine how well it copes with the censored aspect. First, using simulated data with known parameter values, with and without censoring and error, model fitting was conducted to see how reliably and closely the original parameter values were reproduced. This included omitting BLQ values from the fitting, treating them as described above, and by assuming BLQ values are known with the same error distribution as the other data. Second, real data were used with the above described procedure, and by omitting BLQ values, and the corresponding fits compared. In each case, parameter estimates and fitted curves did not significantly differ with the different methodologies. Further, in the simulated data case, the original parameters were closely recovered.

4.3. *Estimation procedure and parameter uncertainty*

Standard numerical optimisation methods were used to find a minimiser $\hat{\mathbf{p}}$ of the negative of the log-likelihood expression (hereafter referred to as the objective function), and the minimiser was used as an estimate of the parameters. See e.g. Seber and Wild [30]. This optimisation was carried out in Mathematica using the `NMinimize` function.

To attempt to quantify the uncertainty in the parameter estimates, the asymptotic (for a large number of observations) distribution of the parameter estimates was found [30]. This technique is appropriate even if $\hat{\mathbf{p}}$ is only a local minimiser of the objective function, rather than a global minimiser.

The asymptotic distribution of the parameter estimate $\hat{\mathbf{p}}$ is approximately MVN$(\mathbf{p}^*, \mathbf{C})$ where MVN denotes the multivariate normal family of distributions, $\mathbf{p}^*$ is the "true" value of $\mathbf{p}$ and the variance-covariance matrix $\mathbf{C}$ is described next. Consider the linear approximation to the dependence of the unweighted residuals on the parameters about the estimate $\hat{\mathbf{p}}$:

$$\mathbf{R}(\hat{\mathbf{p}}) = \frac{\partial}{\partial \mathbf{p}^{\mathrm{T}}}(\tilde{\mathbf{y}} - \mathbf{h}(\mathbf{p}))|_{\mathbf{p}=\hat{\mathbf{p}}}. \tag{12}$$

The inverse of the Fisher information matrix at $\hat{\mathbf{p}}$ provides an estimate $\mathbf{C}$ of the asymptotic variance-covariance matrix for $\hat{\mathbf{p}}$,

$$\mathbf{C} = (\mathbf{R}(\hat{\mathbf{p}})^{\mathrm{T}}\mathbf{V}(\hat{\mathbf{p}})^{-1}\mathbf{R}(\hat{\mathbf{p}}))^{-1}. \tag{13}$$

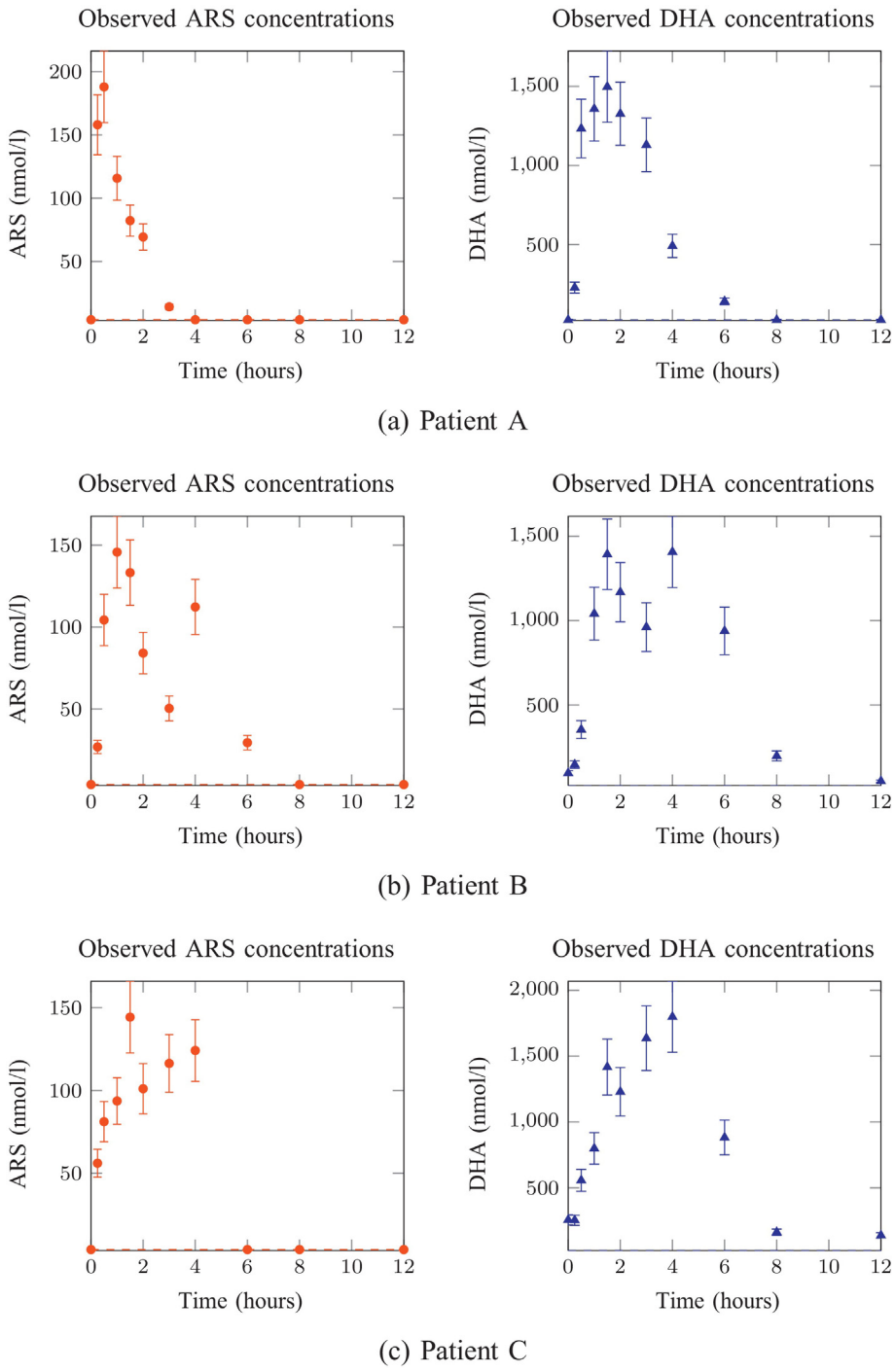

Fig. 2 – Example of observed ARS and DHA plasma concentrations (nmol/l) for three patients. Error bars represent ±15% of the observations and are representative of the assay error (for reasons discussed in Section 4.2).

The variance-covariance matrix **C** is easier to interpret by reporting the diagonal elements of **C** together with the correlation matrix formed by dividing the respective rows and columns by the square roots of these diagonal elements. This information fully specifies **C** but is easier to compare and contrast than **C** itself.

4.4. *Goodness of fit statistics*

Likelihood function values and WRSS values are not directly comparable between patients, due to each data set having a different variation to begin with. Instead, the *(weighted) coefficient of determination* can be used. Loosely speaking, this

expresses the variation in the data explained by the model as a ratio of the total variation present in the data, and is defined as

$$R^2 := 100\left(1 - \frac{(\tilde{\mathbf{y}} - \mathbf{h}(\mathbf{p}))^{\mathrm{T}}\mathbf{V}(\mathbf{p})^{-1}(\tilde{\mathbf{y}} - \mathbf{h}(\mathbf{p}))}{(\tilde{\mathbf{y}} - \bar{\mathbf{y}})^{\mathrm{T}}\mathbf{V}(\mathbf{p})^{-1}(\tilde{\mathbf{y}} - \bar{\mathbf{y}})}\right)\%, \quad (14)$$

where the elements of $\bar{\mathbf{y}}$ are the average of the observed values for the corresponding curve.

The idea is that a larger coefficient of determination should indicate a better fit. However, a large value of this statistic does *not* necessarily correspond to a high likelihood, which is in some ways problematic, but it does accord at least qualitatively with a visual analysis of fits. (Note that the baseline model is simply a mean model, which is not contained in the fitted model class, so the ANOVA interpretation of this statistic does not apply.)

4.5. *Results: individual fits*

Due to the wide range in concentrations reported for individual patients over the studied time interval, parameter fitting using the weighting matrix corresponding to the reported errors did not yield good fits. When using errors corresponding to predicted observations, high concentrations were artificially predicted, corresponding to low weights. These points could thus be missed completely with little penalty on the likelihood. Prior to conducting the analysis, this symptom was expected and it was planned that the condition number of the weighting matrix might need to be controlled to resolve this. The singular values of the weighting matrix (to cater for the cases where the matrix was not diagonal due to the assumption of correlation between different measurement errors) were therefore capped so that no singular value exceeded 100 times the lowest singular value, resulting in the condition number of the weighting matrix becoming at most 100. Imposing this cap yielded much improved model fits.

Even with this cap, the objective function had multiple local minima for many patients, and often had multiple local minima achieving similar objective function values but considerably different parameter estimates. In these cases, the global minimum was usually selected, except in a minority of cases where the fitted parameter values were extreme and a local minimum seemed more realistic. This highlights the fact that having a globally identifiable model structure is a necessary but not sufficient condition to ensure robust parameter estimation from sampled data, especially in the presence of high model and observation errors.

Observations and model fits for the three patients whose profiles were shown previously are presented in Fig. 3 (patient A), Fig. 4 (patient B) and Fig. 5 (patient C), together with model predictions of the quantities in the absorption compartments, and estimated parameter values with measures of their uncertainty. The confidence bands give an indication of the sensitivity of the fit and are explained and discussed in the following section.

It can be seen that the model fit for patient A appears to be satisfactory. It is difficult to determine whether the fit for patient B is reasonable or not because the concentration–time profiles observed are unusual, and may or may not be a result of random measurement error. The fit for patient C is unsatisfactory because the model cannot account for the later peaks due to the model misspecification mentioned earlier. The confidence bands for patient C also clearly indicate a problem with the model.

Table 2 – Fitted parameter values, aggregated

Parameter	Mean (SD)	Units
$b\alpha$	0.4723 (0.3205)	kg/l
r	4.3870 (fixed)	Dimensionless
k_{21}	0.2806 (0.2987)	h^{-1}
k_{42}	1.1185 (0.7436)	h^{-1}
k_{43}	0.8347 (0.5908)	h^{-1}
k_{e4}	1.6123 (1.2848)	h^{-1}
CoD weighted	74.2505 (28.8048)	%
ARS half-life	0.9283 (0.5778)	h
DHA half-life	0.7156 (0.5304)	h

For brevity, results for the other patients are not presented here in the same way, but instead model fit results are summarised through the coefficient of determination and shown in Fig. 6, and a summary of parameter estimates across all patients is provided in Table 2. The worst model fits correspond to patients whose observed ARS and DHA concentration–time profiles did not both reach peaks within 3 h of dose administration, or those where at least one of the drugs exhibited multiple peaks (approximately half of the patients exhibited one of these issues, and are coloured in red in Fig. 6). Note that the fit for one such patient has a negative coefficient of determination. This does not necessarily suggest that fitting the mean to the concentration–time profile of each drug would have performed better than fitting the model (although that is a natural interpretation), because the model still captures part of the absorption and elimination processes and therefore their shapes, though model predictions should not be relied upon in these circumstances. The coefficient of determination statistic was used to help quantify the goodness of the model fits, but it is not without problems and should not be considered the sole determinant of the result.

The fits were typically insensitive to the correlation parameter ρ (perhaps as a result of the weight cap) and this parameter was often fitted close to 0 even when not used as the initial value for the optimisation. Having preferred a local minimum over the global minimum in some cases, no individual parameter estimates were unreasonable in isolation. However, the parameter estimates were not always considered well determined and many varied significantly between patients. This was most marked for k_{21}, where the largest and smallest estimated values differed by a factor of 100, while the other parameters varied by roughly a factor of 10. The wide variability in the patient profiles makes it possible that (though unclear whether) this is plausible, and could be due to differences in the severity of the malaria, issues with the quality of the data, or other covariates (such covariates were not available for evaluation here). These issues will be explored further in the following section, “Sensitivity analysis”.

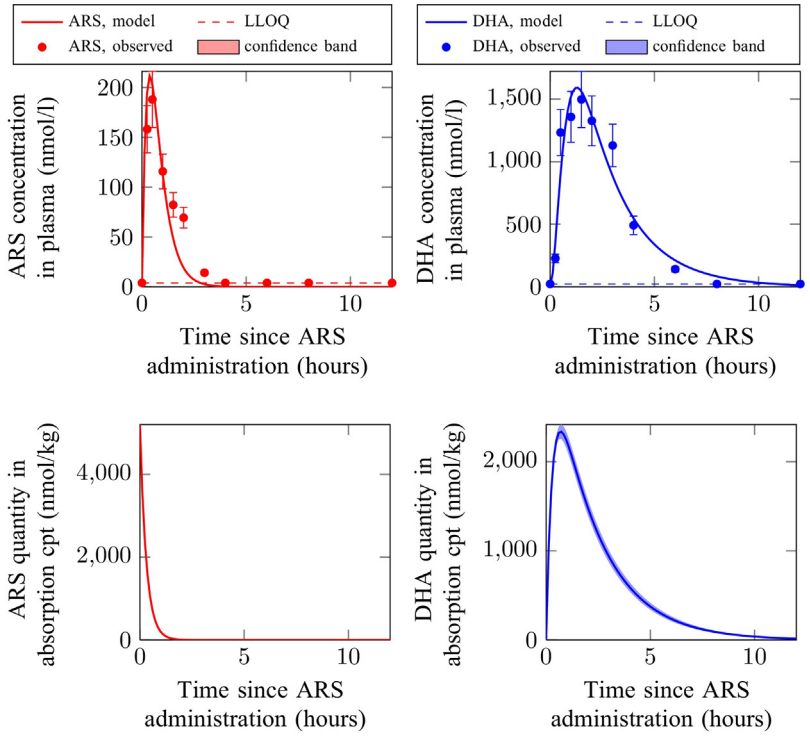

Parameter	Fitted value	Standard error	Units
$b\alpha$	0.2330	0.0105	kg/l
r	4.3870	(fixed)	dimensionless
k_{21}	1.2518	0.0863	h^{-1}
k_{42}	2.0378	0.0199	h^{-1}
k_{43}	0.4604	0.0113	h^{-1}
k_{e4}	0.9975	0.0426	h^{-1}
ρ	0.0207	(nuisance)	correlation
Objective function value	3747.23		
Coefficient of determination	96.46		%

Parameter correlation matrix (darkness of black/red colour corresponds to strength of positive/negative value in each cell respectively):

	$b\alpha$	k_{21}	k_{42}	k_{43}	k_{e4}
$b\alpha$	1.000	−0.977	0.199	−0.767	0.994
k_{21}	−0.977	1.000	−0.292	0.638	−0.982
k_{42}	0.199	−0.292	1.000	−0.021	0.187
k_{43}	−0.767	0.638	−0.021	1.000	−0.712
k_{e4}	0.994	−0.982	0.187	−0.712	1.000

Fig. 3 – Example of model predicted ARS and DHA quantities/concentrations in each compartment for patient A, with table of parameter estimates and their uncertainties. As previously, error bars are representative of assay error.

Many people working in the field prefer to express elimination parameters in terms of half-lives. From the parameters in the parameter vector **p**, the ARS half-life can be calculated as

$$t_{\frac{1}{2},\mathrm{ARS}} = \ln 2/(k_{42} + k_{e2}), \tag{15}$$

and the DHA half-life as

$$t_{\frac{1}{2},\mathrm{DHA}} = \ln 2/k_{e4}. \tag{16}$$

Estimates of these parameters obtained here (shown in Table 2) agree in range with those summarised in Morris et al. [12] (0.36–1.2 h for ARS and 0.49–3.08 h for DHA), but while Morris et al. [12] report that the DHA half-life is consistently longer than that of ARS, the same result was not found for all the patients in this study; the reasons for this are unclear.

Model fitting was also conducted by relaxing one constraint at a time (still resulting in SGI model structures) to assess the effect on the parameter estimates. Doing so either did not significantly alter the parameter estimates, or otherwise did not generally improve fits visually (sometimes making them appear noticeably worse), and only marginally reduced the objective function values. The resulting estimates for some parameters were very close to their constrained values in some cases, while in others, the parameter estimates

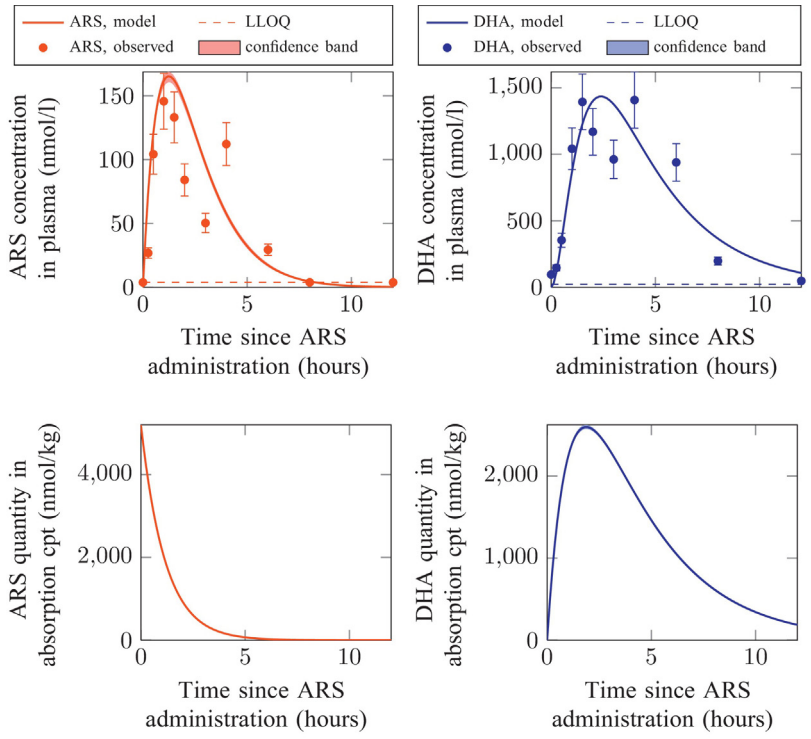

Parameter	Fitted value	Standard error	Units
$b\alpha$	0.6730	0.0205	kg/l
r	4.3870	(fixed)	dimensionless
k_{21}	0.1037	0.0053	h^{-1}
k_{42}	0.7568	0.0104	h^{-1}
k_{43}	0.3020	0.0043	h^{-1}
k_{e4}	1.8599	0.0559	h^{-1}
ρ	0.1809	(nuisance)	correlation
Objective function value	7372.58		
Coefficient of determination	88.75		%

Parameter correlation matrix (darkness of black/red colour corresponds to strength of positive/negative value in each cell respectively):

	$b\alpha$	k_{21}	k_{42}	k_{43}	k_{e4}
$b\alpha$	1.000	−0.917	−0.681	0.245	0.989
k_{21}	−0.917	1.000	0.754	−0.491	−0.935
k_{42}	−0.681	0.754	1.000	−0.764	−0.739
k_{43}	0.245	−0.491	−0.764	1.000	0.362
k_{e4}	0.989	−0.935	−0.739	0.362	1.000

Fig. 4 – Example of model predicted ARS and DHA quantities/concentrations in each compartment for patient B, with table of parameter estimates and their uncertainties. As previously, error bars are representative of assay error.

changed significantly and inconsistently, and their associated uncertainties increased also. When this occurred, the changes propagated to the other parameters too (due to the correlation), resulting in even wider variability of the parameters between patients. These results therefore provide evidence suggesting that the constraints imposed are as reasonable as could be hoped.

5. Sensitivity analysis

A sensitivity analysis was also carried out to assess how well-determined the parameter estimates are (with the exception of the nuisance parameter ρ), and the effects of slight perturbations of parameters on model predictions. This informs on how accurately it is *possible* to determine the parameters and how accurately it is *necessary* to determine them.

The statistical parameter correlation matrices reported together with the parameter estimates contain sensitivity information. They indicate by how much changes in any given parameter will affect the other parameters if the fits are to remain similar. Pairs of parameters which are highly correlated and parameters with high standard errors may be difficult to estimate numerically. Many pairs of the parameters have high correlations, with absolute values above 0.80, and this is one possible explanation for some of the issues

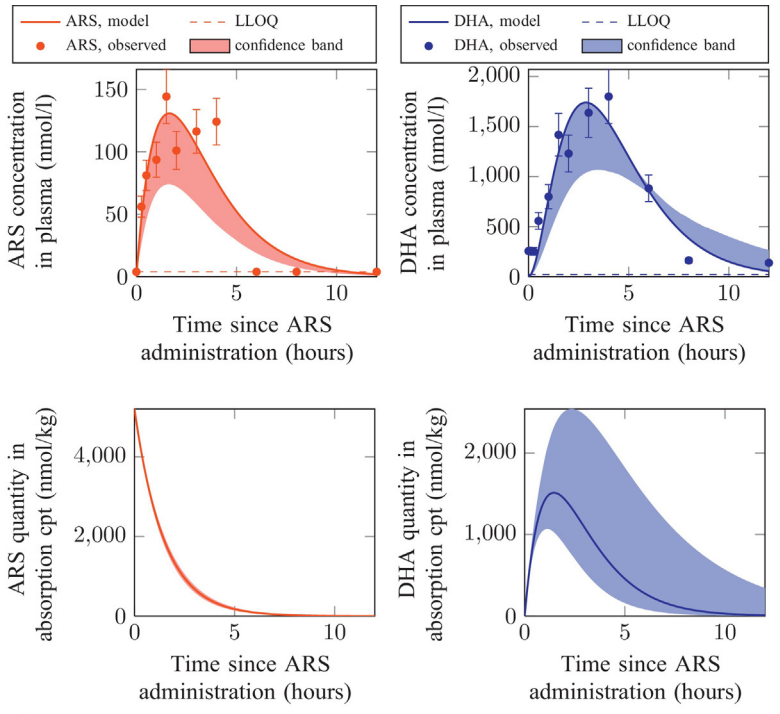

Parameter	Fitted value	Standard error	Units
$b\alpha$	0.3070	0.1294	kg/l
r	4.3870	(fixed)	dimensionless
k_{21}	0.1355	0.0570	h^{-1}
k_{42}	0.5420	0.0306	h^{-1}
k_{43}	0.6935	0.3297	h^{-1}
k_{e4}	0.7576	0.3184	h^{-1}
ρ	0.0010	(nuisance)	correlation
Objective function value	7945.91		
Coefficient of determination	89.62		%

Parameter correlation matrix (darkness of black/red colour corresponds to strength of positive/negative value in each cell respectively):

	$b\alpha$	k_{21}	k_{42}	k_{43}	k_{e4}
$b\alpha$	1.000	−0.996	0.908	−0.997	1.000
k_{21}	−0.996	1.000	−0.877	0.988	−0.996
k_{42}	0.908	−0.877	1.000	−0.937	0.909
k_{43}	−0.997	0.988	−0.937	1.000	−0.997
k_{e4}	1.000	−0.996	0.909	−0.997	1.000

Fig. 5 – Example of model predicted ARS and DHA quantities/concentrations in each compartment for patient C, with table of parameter estimates and their uncertainties. As previously, error bars are representative of assay error.

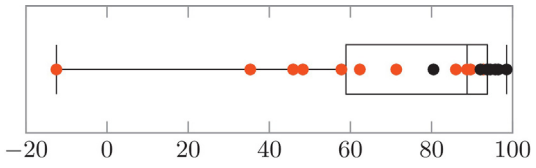

Fig. 6 – Distribution of the coefficient of determination (%) over the dataset; marks in red correspond to patients with unexpected profiles. Recall that the objective was not to maximise the coefficient of determination, but this statistic allows easier comparison between subjects than the actual objective function values.

encountered with the parameter estimation described in the previous section.

The fitted parameters have an asymptotic multivariate normal distribution centred around the fitted values, with variance given approximately by the corresponding dispersion matrix (the matrix formed by the combination of the correlations and the standard errors), and this parameter distribution gives rise to distributions revealing the local uncertainty around the fitted curves. Monte Carlo techniques were used to estimate the 10th and 90th percentiles of the latter distributions, and the regions between these two percentiles form the pointwise confidence/prediction bands illustrated in the plots.

While it has already been noted that this model is not suitable for all patients, particularly due to the issues with the peaks, in many cases where the issue is prominent, the confidence bands indicate that there is an issue with the model (as observed for patient C).

A further analysis was also carried out using normalised (first-order) sensitivities, considering the whole time domain of interest instead of just the observational times as in the statistical results. The sensitivity of a dependent variable x to a change in the parameter p_j (considered about parameter vector $\hat{\mathbf{p}}$) is the local quantity given by [31,32]

$$s_{x,p_j} := \left(\frac{\partial x}{\partial p_j}\right)\Big|_{\hat{\mathbf{p}}},$$

but for comparing between different parameters, the following semi-normalised form is preferred [33]:

$$S_{x,p_j} := \left(p_j \frac{\partial x}{\partial p_j}\right)\Big|_{\hat{\mathbf{p}}},$$

which has the same units as x. Note that this formulation normalises only by the presence of the p_j, and does not divide by x itself (unlike as in [31,32]) to facilitate interpretation in an identifiability and correlation sense.

Note that if the variable x is a function of an independent variable—such as time as here—then so are its sensitivities (S_{x,p_j}). It is therefore useful to summarise each as a single value, in addition to visualising them as graphical plots over the relevant domains. A natural summary is the mean of the absolute value of the sensitivity function,

$$\overline{S_{x,p_j}} := \frac{1}{12}\int_0^{12} |S_{x,p_j}(t)|\,dt. \tag{17}$$

If the shapes of curves (exclusive of direction and scale) for the sensitivities of multiple parameters are similar for all observation variables, or if any parameters have low normalised sensitivities, numerical identifiability of those parameters will be difficult. In this case, if the curves for the corresponding model predictions are not also similar, inability to identify the parameters numerically will have a significant effect on the predictions.

While sensitivity depends on the estimated parameters and so is a local property, when applied to the model presented here, the sensitivity for different patients at their respective parameter estimates were very similar in shape, only with differences in scale; therefore only patient A is reported in full detail. The graphical plots for the normalised sensitivities for patient A are collected in Fig. 7 together with their means as described above. As the observation gain for the observed circulation compartments does not have any relevance to the predicted quantities in the absorption compartments, note that $b\alpha$ has no influence on the latter, which has to be considered modulo the unidentifiable bioavailability factor b.

Recall from earlier that not all parameters were considered well determined by the data for a number of patients.

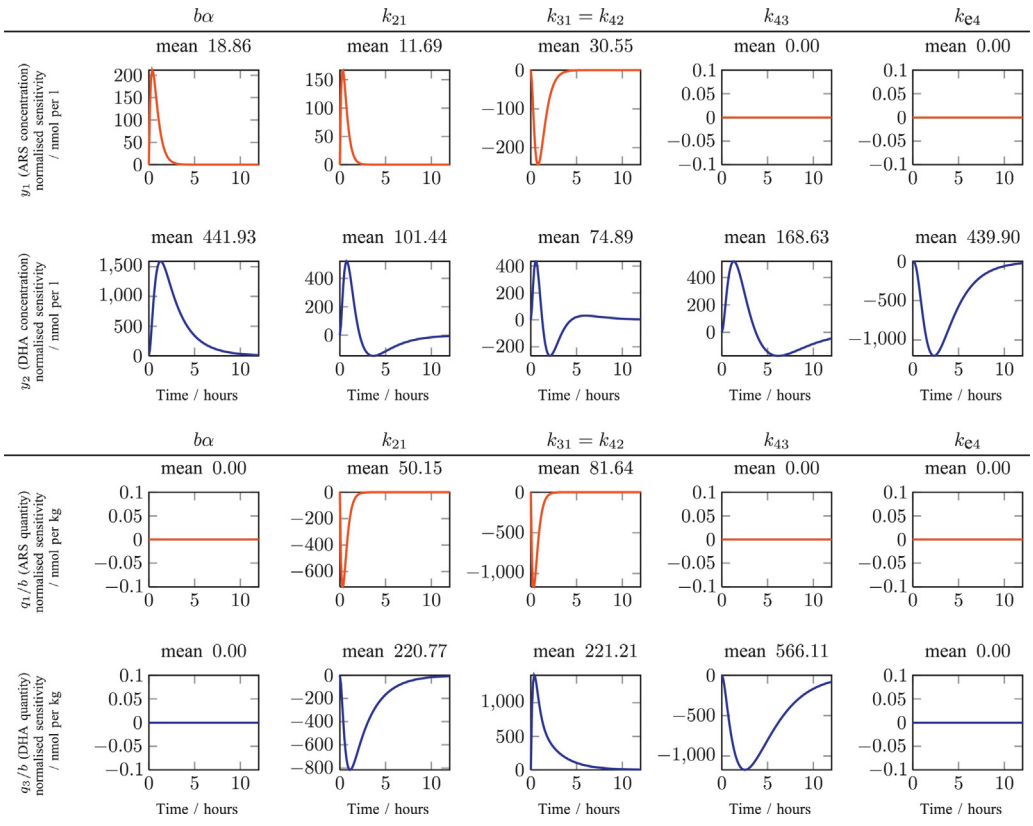

Fig. 7 – Normalised sensitivity plots for the model about the estimated parameters for patient A, first with respect to the observations and then the unobserved compartments

This can now be explored in more depth. Subjects for which such issues were observed had high standard deviation estimates for the problem parameter(s), and had corresponding normalised sensitivities relating to the observed quantities an order of magnitude lower than that shown for patient A. In some cases, when the observations are insensitive to a parameter, the model predictions are similarly insensitive to it as well. Therefore, even though the parameter cannot be estimated to a high degree of confidence in such circumstances, it is not necessary for it to be known with high precision to maintain model utility. On the other hand, there were some parameters to which the unobserved quantities were equally or more sensitive than the observed quantities, and the model is of limited use when these parameters cannot be estimated with confidence, such as in the case of patient C.

6. Conclusion

A novel feature of the proposed model is that it accounts for the possibility that some of the orally administered parent drug ARS is metabolised into DHA before it is completely absorbed, e.g. as a first-pass effect. This is consistent with previous reports in the literature. Just as the pharmacokinetics of ARS and DHA differ widely between individuals, so too do the goodness of fits and parameter estimates under this new model. Model fits appeared to be reasonably good for a number of patients, but the concentration–time profiles for certain patients did not fit the usual absorption behaviour, and model fitting was less satisfactory for some of these patients.

The authors are currently looking into those data sets where double peaks were apparent, and further investigation is also needed with more extensive datasets. If this phenomenon is observed elsewhere and confirmed to be distinct from random measurement error, the authors would like to determine a more appropriate mechanistic model under these circumstances. Future work also includes consideration of optimal design measures and performing a random effects analysis for the subjects—a kind of population analysis, where parameters are estimated using all individual data sets, allowing the parameters to borrow support across all individual data sets while still providing separate fits for each individual patient.

An important influencing factor in the pharmacokinetics of the artemisinin drugs is the severity of the malaria infection in the subject. Specifically, the disposition and effectiveness of artemisinin drugs very much depends on the number of parasites within each of the developmental forms (ring forms, young trophozoites, mature trophozoites and schizonts, etc.) during the therapeutic window, as each stage has a different artemisinin susceptibility and the pharmacodynamic action is a route of elimination for these drugs. Reduced ring form susceptibility is also thought to be an important effect of parasite resistance to artemisinins [19]. Therefore, the authors are currently investigating pharmacokinetic/pharmacodynamic models incorporating the lifecycle of the parasites where the drugs affect the parasites and the parasites affect the drugs.

Conflict of interest statement

None of the authors declare any conflict of interest.

Acknowledgements

This work was supported in part by the Engineering and Physical Sciences Research Council through the MASDOC DTC [grant number EP/HO23364/1].

The authors would like to thank Dr Abhishek Srivastava at the Department of Parasitology at the Liverpool School of Tropical Medicine for assaying the samples, and the patients who all gave written informed consent for the data to be used for any appropriate and ethical research purposes.

The authors would also like to thank the two anonymous reviewers for their helpful comments and suggestions.

REFERENCES

[1] D.A. Joy, X. Feng, J. Mu, T. Furuya, K. Chotivanich, A.U. Krettli, M. Ho, A. Wang, N.J. White, E. Suh, P. Beerli, X.-z. Su, Early origin and recent expansion of *Plasmodium falciparum*, Science 300 (2003) 318–321.

[2] WHO, World Malaria Report 2011, World Health Organization, 2011.

[3] P. Newton, Y. Suputtamongkol, P. Teja-Isavadharm, S. Pukrittayakamee, V. Navaratnam, I. Bates, N. White, Antimalarial bioavailability and disposition of ARS in acute falciparum malaria, Antimicrobial Agents and Chemotherapy 44 (2000) 972–977.

[4] WHO, Guidelines for the treatment of malaria, World Health Organization, 2010.

[5] N. White, Preventing antimalarial drug resistance through combinations, Drug Resistance Updates 1 (1998) 3–9.

[6] K. Starčević, D. Pešić, A. Toplak, G. Landek, S. Alihodžić, E. Herreros, S. Ferrer, R. Spaventi, M. Perić, Novel hybrid molecules based on 15-membered azalide as potential antimalarial agents, European Journal of Medicinal Chemistry 49 (2012) 365–378.

[7] N. Klonis, M.P. Crespo-Ortiz, I. Bottova, N. Abu-Bakar, S. Kenny, P.J. Rosenthal, L. Tilley, Artemisinin activity against *Plasmodium falciparum* requires hemoglobin uptake and digestion, Proceedings of the National Academy of Sciences 108 (2011) 11405–11410.

[8] P.M. O'Neill, V.E. Barton, S.A. Ward, The molecular mechanism of action of artemisinin – the debate continues, Molecules 15 (2010) 1705–1721.

[9] A.N. LaCrue, M. Scheel, K. Kennedy, N. Kumar, D.E. Kyle, Effects of ARS on parasite recrudescence and dormancy in the rodent malaria model *Plasmodium vinckei*, PLoS ONE 6 (2011) e26689.

[10] S. Meshnick, The mode of action of antimalarial endoperoxides, Transactions of the Royal Society of Tropical Medicine and Hygiene 88, Supplement 1 (1994) 31–32.

[11] Q. Cheng, D. Kyle, M. Gatton, Artemisinin resistance in *Plasmodium falciparum*: a process linked to dormancy? International Journal for Parasitology: Drugs and Drug Resistance (2012).

[12] C. Morris, S. Duparc, I. Borghini-Fuhrer, D. Jung, C. Shin, L. Fleckenstein, Review of the clinical pharmacokinetics of ARS and its active metabolite DHA following intravenous, intramuscular, oral or rectal administration, Malaria Journal 10 (2011) 263.

[13] H.J. Woerdenbag, N. Pras, W. van Uden, T.E. Wallaart, A.C. Beekman, C.B. Lugt, Progress in the research of artemisinin-related antimalarials: an update, Pharmacy World & Science 16 (1994) 169–180.
[14] X. Li, A. Björkman, T. Andersson, L. Gustafsson, C. Masimirembwa, Identification of human cytochrome p450s that metabolise anti-parasitic drugs and predictions of in vivo drug hepatic clearance from in vitro data, European Journal of Clinical Pharmacology 59 (2003) 429–442.
[15] N. Lindegårdh, A. Dondorp, P. Singhasivanon, N. White, N. Day, Validation and application of a liquid chromatographic-mass spectrometric method for determination of artesunate in pharmaceutical samples, Journal of Pharmaceutical and Biomedical Analysis 45 (2007) 149–153.
[16] Q. Li, P. Weina, Artesunate: the best drug in the treatment of severe and complicated malaria, Pharmaceuticals 3 (2010) 2322–2332.
[17] K. Batty, T. Davis, L. Thu, T. Quang Binh, T. Kim Anh, K. Ilett, Selective high-performance liquid chromatographic determination of artesunate and α-and β-dihydroartemisinin in patients with falciparum malaria, Journal of Chromatography B: Biomedical Sciences and Applications 677 (1996) 345–350.
[18] E. Scholar, W. Pratt, The Antimicrobial Drugs, Oxford University Press, 2000.
[19] S. Saralamba, W. Pan-Ngum, R.J. Maude, S.J. Lee, J. Tarning, N. Lindegårdh, K. Chotivanich, F. Nosten, N.P.J. Day, D. Socheat, N.J. White, A.M. Dondorp, L.J. White, Intrahost modeling of artemisinin resistance in *Plasmodium falciparum*, Proceedings of the National Academy of Sciences 108 (2011) 397–402.
[20] T. Gordi, R. Xie, N. Huong, D. Huong, M. Karlsson, M. Ashton, A semi-physiological pharmacokinetic model for artemisinin in healthy subjects incorporating autoinduction of metabolism and saturable first-pass hepatic extraction, British Journal of Clinical Pharmacology 59 (2005) 189–198.
[21] B. Tan, H. Naik, I.-J. Jang, K.-S. Yu, L. Kirsch, C.-S. Shin, J. Craft, L. Fleckenstein, Population pharmacokinetics of artesunate and dihydroartemisinin following single- and multiple-dosing of oral artesunate in healthy subjects, Malaria Journal 8 (2009) 304.
[22] H.A. Karunajeewa, K.F. Ilett, K. Dufall, A. Kemiki, M. Bockarie, M.P. Alpers, P.H. Barrett, P. Vicini, T.M.E. Davis, Disposition of artesunate and dihydroartemisinin after administration of artesunate suppositories in children from Papua New Guinea with uncomplicated malaria, Antimicrobial Agents and Chemotherapy 48 (2004) 2966–2972.
[23] J.A. Jacquez, Compartmental Analysis in Biology and Medicine, third edition, BioMedware, Ann Arbor, MI, 1996.
[24] S.A. Cheung, J. Yates, L. Aarons, Structural identifiability of parallel pharmacokinetic experiments as constrained systems, in: D. Feng, J. Zaytoon (Eds.), Modelling and Control in Biomedical Systems 2006, IPV - IFAC Proceedings Volume, Elsevier Science, 2006, pp. 99–104.
[25] K.R. Godfrey, Compartmental Models and Their Application, Academic Press, 1983.
[26] D. Cole, B. Morgan, D. Titterington, Determining the parametric structure of models, Mathematical Biosciences 228 (2010) 16–30.
[27] N. Lindegardh, W. Hanpithakpong, B. Kamanikom, P. Singhasivanon, D. Socheat, P. Yi, A. Dondorp, R. McGready, F. Nosten, N. White, N. Day, Major pitfalls in the measurement of artemisinin derivatives in plasma in clinical studies, Journal of Chromatography B 876 (2008) 54–60.
[28] M. Van Agtmael, C. Van der Graaf, T. Dien, R. Koopmans, C. Van Boxtel, The contribution of the enzymes CYP2D6 and CYP2C19 in the demethylation of artemether in healthy subjects, European Journal of Drug Metabolism and Pharmacokinetics 23 (1998) 429–436.
[29] M. Bergstrand, M.O. Karlsson, Handling data below the limit of quantification in mixed effect models, The AAPS journal 11 (2009) 371–380.
[30] G. Seber, C. Wild, Nonlinear Regression, vol. 503, Wiley, New York, 1989.
[31] H. Banks, S. Dediu, S.L. Ernstberger, F. Kappel, Generalized sensitivities and optimal experimental design, Journal of Inverse and Ill-posed Problems 18 (2010) 25–83.
[32] A. Varma, M. Morbidelli, H. Wu, Parametric Sensitivity in Chemical Systems, Cambridge Series in Chemical Engineering, Cambridge University Press, 2005.
[33] A. Rössler, M. Fink, N. Goswami, J. Batzel, Modeling of hyaluronan clearance with application to estimation of lymph flow, Physiological Measurement 32 (2011) 1213.